Piezoresistive Microcantilevers From Ultrananocrystalline Diamond

Natalya L. Privorotskaya, Hongjun Zeng, *Senior Member, IEEE*, John A. Carlisle, Rashid Bashir, *Fellow, IEEE*, and William P. King, *Member, IEEE*

***Abstract*—This paper reports on the temperature-dependent electrical resistivity and piezoresistive characteristics of boron-doped ultrananocyrstalline diamond (UNCD) and the fabrication of piezoresistive microcantilevers using boron-doped and undoped UNCD. The devices consist of 1-μm-thick doped UNCD on either 1- or 2-μm-thick undoped UNCD. The electrical resistivity of doped UNCD is 0.1 $\Omega \cdot$ cm at room temperature, which is five orders of magnitude smaller than the electrical resistivity of undoped UNCD. Over the temperature range of 25 °C–200 °C, the doped UNCD has a temperature coefficient of electrical resistance of (-1.4×10^{-3}) per °C. The doped UNCD exhibits a significant piezoresistive effect with a gauge factor of 7.53 $\pm$ 0.32 and a piezoresistive coefficient of 8.12×10^{-12} Pa^{-1} at room temperature. The piezoresistive properties of UNCD are constant over the temperature range of 25 °C–200 °C. Microcantilevers having a length of 300 μm have a deflection sensitivity of 0.186 mΩ/Ω per micrometer of cantilever end deflection. These measurements of electrical and piezoresistive properties of doped UNCD could aid the design of future diamond microsystems. [2010-0020]**

***Index Terms*—Diamond, microcantilever, piezoresistivity.**

I. Introduction

PIEZORESISTIVE microcantilevers have been used in both atomic force microscopy (AFM) and biochemical detection [1]–[3]. In a piezoresistive cantilever, cantilever deflection is sensed via strain-dependent cantilever electrical resistance [4], [5]. Most piezoresistive microdevices have been based on silicon because of the large piezoresistive effect in doped silicon and well-established silicon fabrication processes. The disadvantages of silicon piezoresistive cantilevers are that silicon is not biocompatible, it does not dissolve in water and aqueous solutions, and its piezoresistive coefficient is strongly temperature dependent [6], [7]. Recent advances in chemical vapor deposition (CVD) diamond film technology have shown diamond to be an attractive alternative to silicon for microsystem applications [8]–[10]. Diamond is chemically stable, and it has a biochemical compatibility that exceeds that of silicon [11]. This paper reports on the piezoresistive cantilevers that are fabricated entirely out of doped and insulating CVD diamond films.

Ultrananocrystalline diamond (UNCD) is a polycrystalline diamond material with a very high structural uniformity that results from a small grain size, which is around 2–5 nm [12]. Unlike microcrystalline diamond, which can be highly graphitic, UNCD is 95% or more sp^3 bonded, which gives it chemical, mechanical, and electrical properties that are close to those of bulk diamond [13], [14]. The electrical properties of UNCD can be modulated via doping [15], with electrical resistivity that can be controlled over five orders of magnitude. UNCD films can be synthesized at temperatures that are as low as 400 °C, while film thickness can vary from several nanometers to tens of micrometers [16], [17]. Published works on the characterization of UNCD films report on the mechanical [13] and thermal [18] properties at room temperature. However, little work has been published on the temperature dependence of UNCD properties. In particular, temperature-dependent electrical resistivity has not been reported for doped UNCD.

Polycrystalline diamond has been used for microelectromechanical systems (MEMS), including piezoresistive [19] and chemical sensors [20]. Piezoresistive microcantilevers have been made from polycrystalline [21] and highly oriented diamond [22]. Typically, a thin layer of diamond is deposited on top of silicon and is then patterned in desired regions. Silicon is then etched away to produce released membranes or cantilevers [23]. The integrated piezoresistive elements can be fabricated by selective boron doping. While most published works on diamond microcantilevers have focused on diamond integration onto a silicon element, some works have been published on an all-diamond piezoresistive microcantilever from microcrystalline diamond [21], [22]. Atomic force microscope cantilevers made entirely from insulating UNCD have also been reported [24]. However, no published article reports on the integration of doped UNCD with undoped UNCD into a functional microelectromechanical device. Furthermore, the piezoresistive effect in doped UNCD and its dependence on temperature remain unexplored.

The piezoresistive sensitivity of a microcantilever can be characterized by the gauge factor K, defined in terms of the

Manuscript received January 19, 2010; accepted July 14, 2010. Date of publication September 9, 2010; date of current version October 1, 2010. Subject Editor M. Mehregany.

N. L. Privorotskaya is with the Department of Mechanical Science and Engineering, University of Illinois at Urbana–Champaign, Urbana, IL 61801 USA (e-mail: nprivor2@illinois.eud).

H. Zeng and J. A. Carlisle are with Advanced Diamond Technologies, Romeoville, IL 60446 USA (e-mail: zeng@thindiamond.com; carlisle@thindiamond.com).

R. Bashir is with the Department of Electrical and Computer Engineering and Bioengineering and the Micro and Nanotechnology Laboratory, University of Illinois at Urbana–Champaign, Urbana, IL 61801 USA (e-mail: rbashir@illinois.edu).

W. P. King is with the Department of Mechanical Science and Engineering and the Micro and Nanotechnology Laboratory, University of Illinois at Urbana–Champaign, Urbana, IL 61801 USA (e-mail: wpk@uiuc.edu).

Color versions of one or more of the figures in this paper are available online at http://ieeexplore.ieee.org.

Digital Object Identifier 10.1109/JMEMS.2010.2067201

measured resistance change ΔR, unstrained device resistance R, and applied strain ε as

$$K = \frac{\Delta R}{R}\frac{1}{\varepsilon}. \tag{1}$$

The gauge factors are direction dependent, with longitudinal K_L and transverse K_T piezoresistive effects observed when the current is parallel and perpendicular to the applied stress, respectively. K_L for diamond has been measured in the range of 2–1000 [19], [25], while K_T is only a fraction of that value [19], [26]. In general, piezoresistivity in polycrystalline diamond greatly depends on the doping concentration [19], [25], [27], [28], temperature [19], [25], [29], and grain size [21], [28]. Despite the progress in the characterization of diamond and diamond-based structures, no published work reports on the gauge factor of piezoresistive UNCD cantilevers.

This paper reports on the integration of undoped and doped UNCDs into an all-diamond MEMS, investigates on the piezoresistive effect in these UNCD microcantilevers, and reports on the gauge factor of the UNCD material as well as cantilever deflection sensitivity measurements of up to 200 °C. Temperature-dependent resistivity in the same temperature range is measured to complete the analysis.

II. Fabrication

Fig. 1(a) shows the cantilever design concept for a piezoresistive UNCD microcantilever, where the cantilever consists of a layer of doped conducting UNCD layer on top of nonconducting undoped UNCD. A layer of silicon dioxide isolates the undoped UNCD from the silicon handle wafer. Fig. 1(b) also shows the finite element analysis of the cantilever, described later in the paper. We consider four different cantilever designs and cantilever thicknesses of either 2 or 3 μm, resulting in a total of eight device types. Thinner cantilevers are composed of a 1-μm-thick doped UNCD on top of a 1-μm undoped UNCD, while the 3-μm-thick devices have a 1-μm-thick doped UNCD on top of a 2-μm-thick undoped UNCD. This two-layer heterostructure of conducting UNCD on insulating UNCD enables the cantilever to have an electrical resistance change with cantilever deflection. The cantilevers vary in length from 300 μm to 400 μm and have a notch that extends 1/3 or 2/3 of the length, starting from the cantilever substrate. The notched region is referred to as the "leg," while the rest of the cantilever is the "tip."

Fig. 2 shows the cantilever fabrication process, which starts with a diamond-on-insulator wafer having either a 2- or a 3-μm-thick UNCD device bilayer, depending on the cantilever type being made. The UNCD is grown onto a 1-μm-thick silicon dioxide layer on top of a 400-μm-thick silicon handle wafer. The UNCD film was deposited using hot-filament CVD with methane/hydrogen chemistry and a 5% CH_4/H_2 gas mixture. The boron-doped UNCD was synthesized by adding trimethylboron $[B(CH_3)_3]$ as a source gas, with a boron-to-carbon ratio of 1/330, which is inclusive of both carbon-containing source gasses.

We conducted four-point probe measurements on both the undoped and doped UNCD films using an Accent HL5500PC

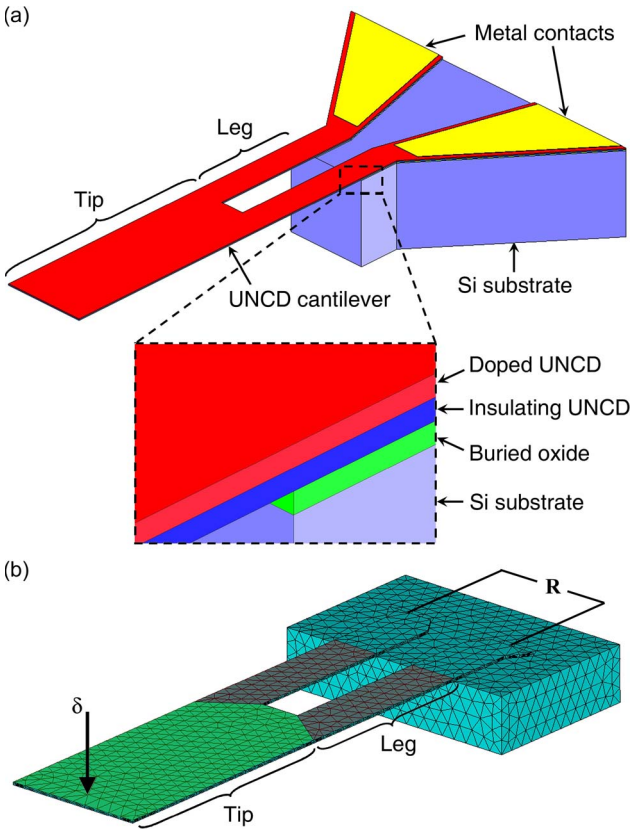

Fig. 1. (a) Schematic view of an all-diamond cantilever with doped and insulated UNCD layers for the measurement of the piezoresistive effect in UNCD. (b) Finite element simulation mesh showing the "leg" and "tip" regions used in the analysis of the piezoresistive effect. The probe location and applied displacement δ are shown at the cantilever free end. The resistance R is obtained using ANSYS electrothermal simulation.

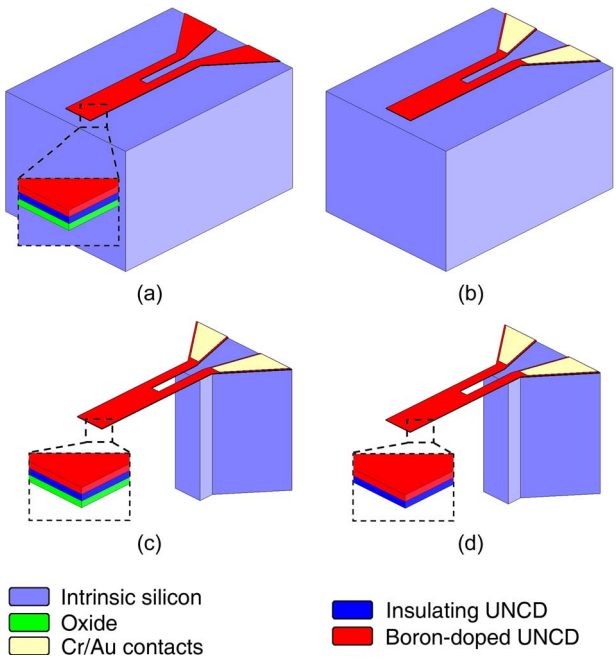

Fig. 2. Fabrication process for the piezoresistive UNCD cantilevers. (a) Beam formation. (b) Metallization. (c) Backside through wafer etch. (d) Oxide etch/final release.

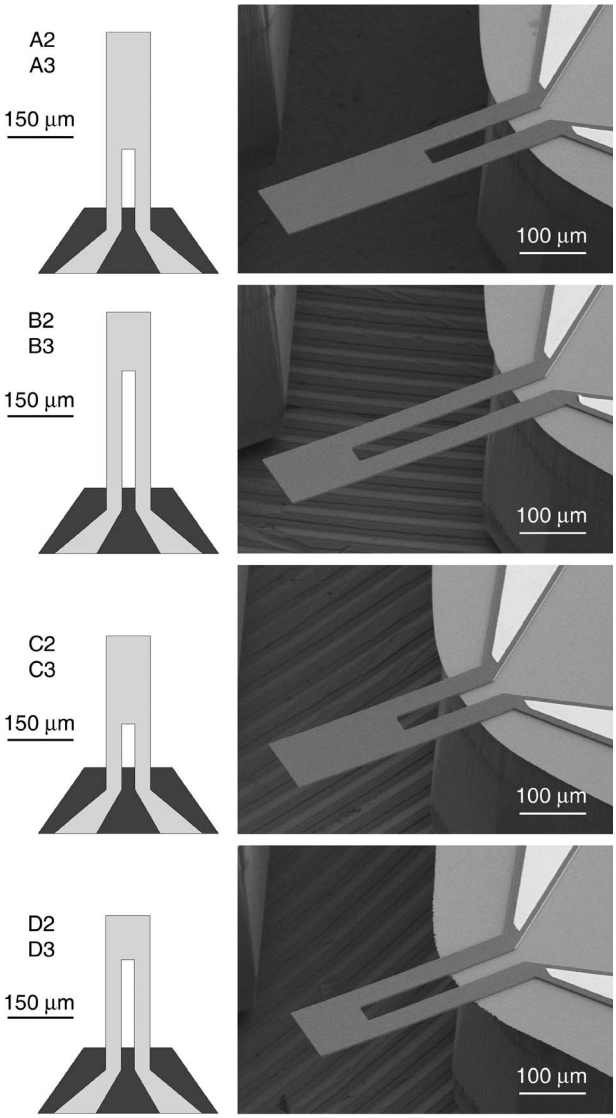

Fig. 3. SEMs of the finished UNCD cantilevers. The image on the left shows the relative dimensions of each cantilever. The SEM images are shown for 3-μm-thick cantilevers.

Hall Effect Measurement System. The sheet resistance of the undoped UNCD was higher than the measurement limit of this apparatus, which is 1 M$\Omega/\square$. Based on the geometry of the sample and measurement system, we conclude that the resistivity of the undoped UNCD is higher than 200 $\Omega \cdot$ cm. The resistivity may be much higher than this lower bound as the typical electrical resistivity for the undoped UNCD synthesized at Advanced Diamond Technologies is above 10^4 $\Omega \cdot$ cm. This high resistivity of the undoped diamond is expected as the UNCD is almost entirely sp^3 bonded. Using the same apparatus, the resistivity of the doped UNCD was measured to be $(91.1 \pm 0.3) \times 10^{-3}$ $\Omega \cdot$ cm. More rigorous measurements of the resistivity of the doped UNCD are presented later in this paper, but at this point, we conclude that the undoped UNCD has an electrical resistivity that is at least four orders of magnitude higher than the undoped UNCD. The Raman spectra of both doped and undoped UNCDs revealed peaks at 1332 and 1560 cm^{-1}, and the Raman spectra was very similar to the published Raman spectra on UNCD [16], [30], [31].

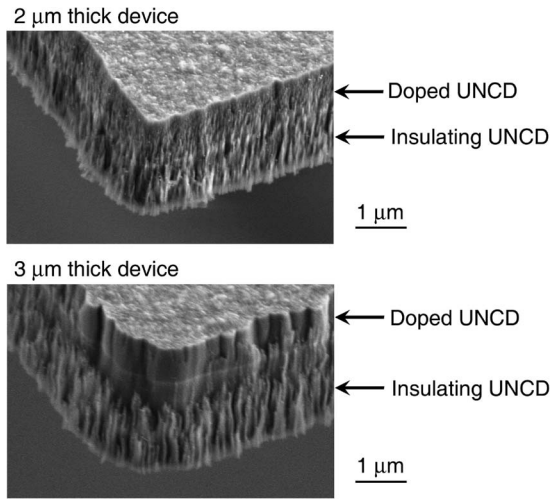

Fig. 4. Zoomed-in view of the (top) 2- and (bottom) 3-μm-thick cantilevers. The top 1-μm layer is boron doped, while the rest of the structure is made from insulating UNCD, which is required in order to measure the piezoresistive effect.

In order to pattern the UNCD cantilever structure, the UNCD layers are etched using reactive ion etching (RIE) with a silicon dioxide mask and an O_2 plasma [Fig. 2(a)]. The 220 nm of Au sputtered on top of a 10-nm Cr adhesion layer forms an ohmic contact to diamond [32]. Metal wet etching defines the contact size and geometry [Fig. 2(b)]. The cantilevers are released via through-wafer etching from the handle wafer backside [Fig. 2(c)], followed by a short HF dip to remove any exposed silicon dioxide [Fig. 2(d)]. About 200 cantilevers can be batch fabricated on one 100-mm-diameter wafer.

Fig. 3 shows the scanning electron micrographs (SEMs) of the fabricated cantilevers. Each cantilever type is named A, B, C, or D, followed by a number that gives the cantilever total thickness. Thus, cantilever "A2" is the "A" design with a 1-μm-thick insulating UNCD and a 1-μm-thick conducting UNCD. The A and B cantilevers are 400 μm long, while the C and D devices have an overall length of 300 μm. The notch extends either 1/3 (cantilevers A and C) or 2/3 (B and D designs) of the total cantilever length, starting at the base. The cantilevers exhibit a slight curvature due to the intrinsic differential stress introduced during the growth process. The cantilever upward tip deflection was about 23 and 16 μm for the 2- and 3-μm-thick 400-μm-long cantilevers, respectively, indicating that the stress does not significantly change between cantilevers with similar thicknesses. Fig. 4 shows an SEM of the cantilever sidewall, where there is a clear distinction between the boron-doped (upper) and insulating (bottom) UNCD layers. The increased sidewall roughness is observed due to the tapering of the sidewall during the RIE etching of diamond. The observed microstructure is due to the RIE etch and is not indicative of the nanometer-scale morphology of UNCD. Table I shows the geometry details and resonant frequencies for the representative cantilevers. The cantilever spring constant could not be precisely determined from AFM, but it is estimated to be 1–9 N/m from calculations and from the measured resonant frequency.

In order to fully characterize the cantilevers, we measured the cantilever electrical resistance during the bending experiments,

TABLE I
SUMMARY OF THE DEFLECTION SENSITIVITY AND GAUGE FACTOR RESULTS FOR EIGHT CANTILEVER TYPES ALONG WITH THEIR DIMENSIONS, RESONANT FREQUENCY, AND RESISTANCE

Cantilever type	Total length, μm	Leg length, μm	Total thickness, μm	Resonant frequency, kHz	Cantilever resistance, kΩ	Deflection Sensitivity, mΩ/ Ω-μm	Gauge Factor
A2	411	144	2.1	21.28±0.002	9.2	0.062±0.001	7.92±0.08
B2	412	276	2.1	21.36±0.002	16.3	0.047±0.001	7.80±0.19
C2	318	116	2.1	35.88±0.001	7.7	0.093±0.004	7.37±0.29
D2	305	205	2.1	38.06±0.001	12.5	0.075±0.003	7.05±0.26
A3	413	145	3.0	31.37±0.003	9.4	0.108±0.002	7.75±0.12
B3	412	277	3.0	31.58±0.004	16.6	0.080±0.001	7.35±0.06
C3	309	110	3.0	56.35±0.001	7.5	0.186±0.003	7.71±0.11
D3	306	205	3.0	54.13±0.002	12.7	0.140±0.001	7.32±0.04

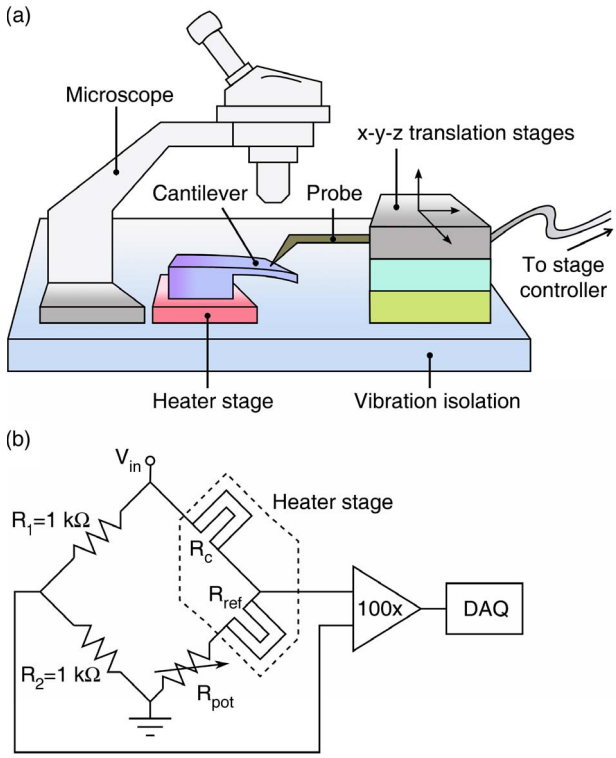

Fig. 5. Schematic showing the experimental setup for piezoresistivity measurements and showing the (a) cantilever deflection setup and (b) cantilever wiring diagram.

which provided a direct measure of cantilever bending sensitivity. To further characterize the gauge factor, we made independent measurements of UNCD resistivity using the van der Pauw structures fabricated alongside the cantilevers and combined these resistivity measurements with the detailed electromechanical finite element simulations and data from the cantilever measurements.

III. EXPERIMENTAL SETUP

Fig. 5(a) shows the overall experimental setup that is used to test the cantilever piezoresistive sensitivity, in which cantilever bending is controlled using a nanopositioner. Each cantilever is a two-terminal device, and wire bonds are made to the two metal terminals in ohmic contact with the doped UNCD. The cantilever resistance R is measured across these terminals, as shown in Fig. 1(b). Two cantilevers are wired into a Wheatstone bridge, in close proximity to each other in order to cancel out the effects of environmental changes and any self-heating [Fig. 5(b)]. The output signal is amplified 100 times and is collected by a data acquisition system. While the cantilever chip position is fixed on the circuit board, a tungsten needle probe with a 5-μm tip radius is allowed to move in three orthogonal directions via motorized nanopositioner stages having a 7-nm resolution. The probe is guided into contact with the cantilever free end under the microscope. The contact can be verified through visual inspection and through changes in the output signal. The location of the probe is measured under a microscope with 150× total magnification. The closed-loop control of the nanopositioner allows for the cantilever bending to be carefully controlled to within 50 nm of vertical deflection. The cantilevers were mounted on a temperature-controlled stage to measure the temperature dependence of piezoresistivity. The heater stage was capable of maintaining temperature to within 0.2 °C in the range of 25 °C–200 °C.

The cantilever resistance change was measured from the Wheatstone bridge voltage output when the applied bridge bias was 1 V. The probe deflection varied from 6.87 to 68.66 μm in 13.73-μm increments, except for the first step of 6.87 μm. Sixty differential voltage measurements were made at each deflection point in 1-s intervals and were repeated three times for averaging purposes and for correcting the signal drift. This procedure was repeated three times, with the probe lifted off the cantilever surface and brought back into contact between subsequent trials to establish uncertainty due to the probe location. While the cantilever resistance could be measured directly from the metal contacts to the cantilever device, additional analysis and measurements were required to determine the cantilever gauge factor. The next sections describe the finite element simulations and electrical resistivity measurements, made independently from the aforementioned cantilever measurements.

IV. Finite Element Simulations

From (1), the gauge factor is a function of the cantilever strain, its initial resistance, and resistance change due to the applied deformation. The cantilever electrical resistance change is measured directly at the electrical contacts on the cantilever, and so this measurement includes both the cantilever and the electrical contacts. The finite element analysis calculates the cantilever initial resistance as well as the strain. Separate structural and electrical models are configured in ANSYS to determine the strain and the room temperature resistance, respectively. The cantilever and part of the substrate are modeled in each case, with the bottom and back faces of the anchor fixed. The cantilever portion consists of two layers having the properties of the doped and insulating UNCDs and having the dimensions of the actual devices. In each model, the cantilever is divided into two regions along the direction of the length of the cantilever: The "leg" region extends from the fixed substrate to the length of the notch, while the "tip" area comprises the rest of the cantilever. Fig. 1(b) shows a typical mesh with 5-μm element size. The mesh convergence study was performed in order to obtain accurate results.

In structural simulations, the cantilever substrate is fixed, and a point load in the form of a known deflection is applied at the probe location measured from the experimental setup. The strain in both longitudinal and transverse directions in the leg and tip regions can then be extracted as volume integrals within the conductive part of the device. The electrical model provides values of the initial resistance in both areas of interest based on the geometry, measured electrical resistivity, and thermal conductivity reported in the literature [18]. Only the conductive layer is considered for resistance calculation as the piezoresistive effect is assumed to come primarily from this part of the structure.

V. Cantilever Deflection Sensitivity

The cantilever deflection sensitivity S can be defined as

$$S = \frac{\Delta R}{R}\frac{1}{\delta} \tag{2}$$

where ΔR is the electrical resistance change relative to the initial resistance R due to the applied cantilever tip deflection δ. For small deflections, deflection sensitivity is directly proportional to the stiffness of the cantilever and depends on the location of the piezoresistor with respect to the neutral axis. Thus, deflection sensitivity is a strong function of geometry.

The deflection of the cantilever free end was determined from the measured probe displacement and the measured probe-cantilever contact point combined with the beam bending theory [33]. Since the cantilever is not a simple rectangular beam, the beam bending theory was compared to finite element analysis to determine the relationship between the location of the contact between the probe tip and cantilever, the probe tip motion, and the deflection at the cantilever free end. The analytical and finite element results agreed to within 1%.

Fig. 6 shows the measured cantilever relative resistance change as a function of the cantilever end deflection. The

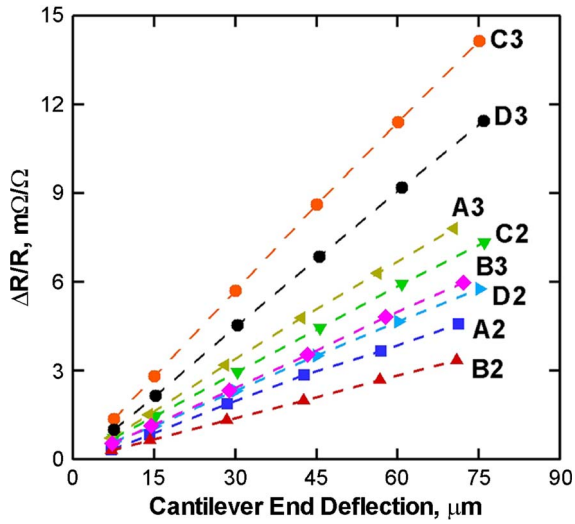

Fig. 6. Relative resistance change as a function of the cantilever end deflection. The deflection sensitivity varies from 0.047 to 0.186 depending on the cantilever geometry. The latter value is only slightly smaller than that for standard silicon cantilevers.

resistance change is linear over the entire range of deflections, with the slope corresponding to the deflection sensitivity in the range of 0.047–0.186 mΩ/Ω per micrometer of deflection. The sensitivity of similarly sized silicon piezoresistive cantilevers is about 0.3 m$\Omega/\Omega \cdot \mu$m[6], [7]. The error bars show the uncertainty in voltage measurements due to electrical noise in the system. Table I summarizes the cantilever deflection sensitivity results along with the measured geometry, measured cantilever resonant frequency, and initial resistance data from electrical finite element simulation for all cantilevers.

The difference in deflection sensitivity values between cantilevers is attributed to the geometry variations. Long cantilevers (A2, A3, B2, and B3) and devices with large notch (B2, B3, D2, and D3) are softer than the shorter versions with the same geometry, resulting in lower deflection sensitivity. Longer cantilevers would however have higher force sensitivity. In addition, the conductive portion of 3-μm cantilevers is located farther away from the neutral axis of the device as compared to 2-μm cantilevers. The doped UNCD layer in the 3-μm cantilevers experience a greater strain than the doped UNCD layer in the 2-μm cantilevers, which translates to a larger observed resistance change. Overall, short and thick cantilevers with a small notch and a piezoresistor restricted to the top surface of the device are preferred for high deflection sensitivity. A thinner layer of UNCD would result in even larger cantilever sensitivity, which could be desired in some applications. However, the measured sensitivity of the present devices was large enough to accurately measure the electrical and piezoresistive properties of the UNCD.

VI. UNCD Resistivity Measurements

The electrical resistivity of UNCD was needed before the cantilever gauge factor could be analyzed. In order to determine the UNCD electrical resistivity, we fabricated van der Pauw structures [34] into the doped UNCD, shown in Fig. 7(a). These structures were fabricated alongside the cantilevers, on

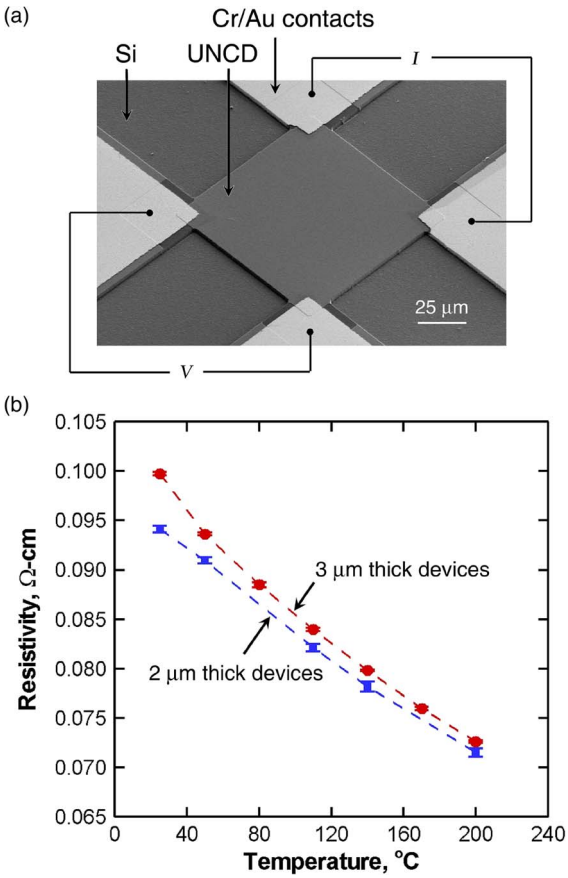

Fig. 7. (a) Structure used for the van der Pauw resistivity measurements showing the probe locations and (b) measurement results for (squares) 2- and (circles) 3-μm UNCD stacks at different temperatures.

the same wafers, and during the same fabrication process. Four square membranes were fabricated on the wafer, with lateral dimensions ranging in size from 100 to 400 μm. These structures were fabricated on the same wafers as the cantilevers such that the layer thicknesses and properties as well as the fabrication process are identical to that of the cantilevers. Eight resistance measurements were performed on each structure type. First, 10 μA of current was applied to two contacts, while the voltage drop was measured across the two remaining metal pads. The same procedure was then repeated with perpendicularly oriented contacts as well as by switching measurement polarity. With a 10-μA test current, resistive heating was less than 0.3 μW, which leads to a negligible temperature rise.

The sheet resistance of the UNCD R_s is given by

$$\exp\left[-\frac{\pi R_{\text{vert}}}{R_s}\right]+\exp\left[-\frac{\pi R_{\text{horiz}}}{R_s}\right]=1 \tag{3}$$

where R_{vert} and R_{horiz} are the average resistances between two vertically and horizontally oriented contacts [34]. The UNCD electrical resistivity $\rho = R_s t$, with t being the thickness of the doped layer measured using SEM. This measurement was repeated over the temperature range of 25 °C–200 °C to establish the temperature–resistivity relationship.

Fig. 7(b) shows the measured UNCD electrical resistivity over the temperature range of 25 °C–200 °C. At 25 °C, the resistivity of UNCD was $(94.1 \pm 0.4) \times 10^{-3}\ \Omega \cdot$ cm for the 2-μm devices and $(99.7 \pm 0.2) \times 10^{-3}\ \Omega \cdot$ cm for the 3-μm devices. These values are comparable to those reported in the literature on polycrystalline and nanocrystalline diamond [35], [36]. The negative temperature coefficient of resistance may be due to the increase in carrier concentration resulting from thermal activation of electrons at higher temperatures.

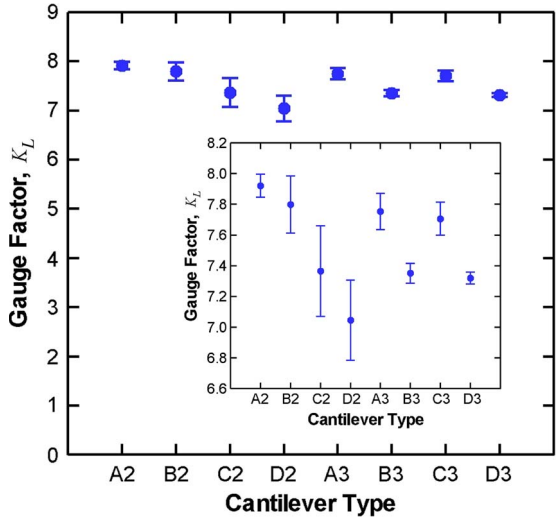

Fig. 8. Measured gauge factor for eight cantilever types, with the inset showing the zoomed-in data. The average gauge factor of UNCD is 7.53 ± 0.32.

VII. Gauge Factor and Piezoresistive Coefficient

While deflection sensitivity depends on cantilever geometry, the longitudinal gauge factor K_L is a material property. Once this property is known, it can be used to predict the piezoresistive response of a device made from a particular material and applied to a device of any size or shape. We assume that transverse deflection is very small since the cantilevers are long, narrow, and thin. K_L is related to the deflection sensitivity of the cantilever through the longitudinal strain in the leg region $\varepsilon_{\text{leg},l}$ and transverse strain in the cantilever free end $\varepsilon_{\text{tip},t}$ as

$$K_L = \frac{\Delta R}{R}\frac{1}{\varepsilon} = \frac{\Delta R}{R_{\text{leg}}\varepsilon_{\text{leg},l} + R_{\text{tip}}\varepsilon_{\text{tip},t}} = \frac{S\delta}{\varepsilon}. \tag{4}$$

The cantilever gauge factor is calculated from the cantilever measurements, and the strain is derived from the structural simulation described earlier. While ΔR and R were directly measured from the metal contacts fabricated into the cantilever device, R_{leg} and R_{tip} were resolved from these measurements, combined with the measurements of resistivity and the finite element simulations.

Fig. 8 shows the gauge factor values calculated for each cantilever type. The average value is 7.53 ± 0.32, which is well within the published data for polycrystalline diamond [19], [21]–[23], [25]. The gauge factor is consistent across all cantilever types and two layer thicknesses, which supports the validity of our overall approach in extracting material properties rather than geometry-specific effects. The error bars in Fig. 8 show the variation within three measurements on the same cantilever when the probe was lifted off the surface and

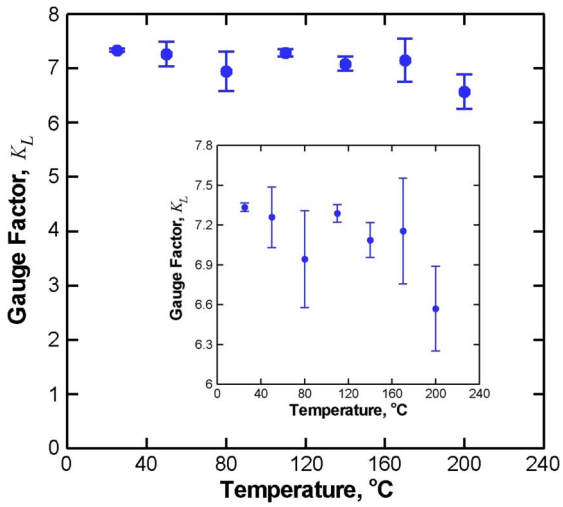

Fig. 9. UNCD gauge factor dependence on temperature, with the inset showing the zoomed-in data. The gauge factor remains constant up to 200 °C.

repositioned between each test. The probe location must be tightly controlled to accurately estimate the gauge factor using this technique. A 10-μm uncertainty in probe location results in as much as ± 0.39 variation in K_L. The UNCD cantilever gauge factor is approximately five times smaller than polycrystalline silicon and 16 times smaller than a single crystal silicon [37]. The UNCD gauge factor is more than double the gauge factor of metals, where most of the effect comes from dimensional changes induced by deformation [37].

Fig. 9 shows the UNCD cantilever gauge factor over the temperature range 25 °C–200 °C for cantilever C3, which was chosen due to its high deflection sensitivity. The gauge factor was constant over the measured temperature range. A slight deviation is seen at 200 °C due to the substantial increase in cantilever noise. While the UNCD piezoresistor response was nearly constant up to 200 °C, the gauge factor in p-type polycrystalline silicon doped to 10^{20} cm^{-3} decreases by 28% over the same temperature range [37].

The cantilever piezoresistive coefficient π_l is related to the gauge factor through Young's modulus and Poisson's ratio according to $K_l = 1 + 2\nu + E\pi_l$. By assuming that the UNCD has a Young's modulus of 790 GPa and a Poisson's ratio of 0.057 [13], the UNCD cantilever piezoresistive coefficient is approximately 8.12×10^{-12} Pa^{-1}. This is 60 times smaller than polycrystalline silicon and about 100 times smaller than single crystal silicon [37].

VIII. Conclusion

In summary, we have shown that the UNCD bilayer heterostructures can be fabricated into an all-diamond microcantilever. The large difference between the doped and undoped UNCDs allows such a structure to be used for piezoresistive measurements. We have designed and fabricated eight types of all-diamond cantilevers to measure the gauge factor at temperatures of up to 200 °C. The cantilevers had measured deflection sensitivity of up to 0.19 mΩ/Ω per micrometer of end deflection. Using separate microstructures, we have measured the electrical resistivity of doped UNCD and its dependence on temperature. Combining the measurements of cantilever behavior with the measurements of electrical resistivity and finite element simulations, we have calculated the room temperature gauge factor of UNCD as 7.53 ± 0.32. Unlike single crystal and polycrystalline silicon, the temperature coefficient of piezoresistivity for UNCD is close to zero. This type of all-UNCD microelectromechanical structure could be used in applications that benefit from the exceptional properties of UNCD, such as biocompatibility, corrosion resistance, and hardness.

References

[1] M. Tortonese, "Force sensors for scanning force microscopy," Ph.D. dissertation, Stanford Univ., Stanford, CA, 1993.
[2] R. Raiteri, M. Grattarola, H.-J. Butt, and P. Skladal, "Micromechanical cantilever-based biosensors," *Sens. Actuators B, Chem.*, vol. 79, no. 2/3, pp. 115–126, Oct. 2001.
[3] H. P. Lang, M. Hegner, and C. Gerber, "Cantilever array sensors," *Mater. Today*, vol. 8, no. 4, pp. 30–36, Apr. 2005.
[4] M. Tortonese, H. Yamada, R. C. Barrett, and C. F. Quate, "Atomic force microscopy using a piezoresistive cantilever," in *Proc. Transducers*, 1991, pp. 448–451.
[5] A. A. Barlian, W.-T. Park, J. R. Mallon, Jr., A. J. Rastegar, and B. L. Pruitt, "Review: Semiconductor piezoresistance for microsystems," *Proc. IEEE*, vol. 97, no. 3, pp. 513–552, Mar. 2009.
[6] B. W. Chui, L. Aeschimann, T. Akiyama, U. Staufer, N. F. de Rooij, J. Lee, F. Goericke, W. P. King, and P. Vettiger, "Advanced temperature compensation for piezoresistive sensors based on crystallographic orientation," *Rev. Sci. Instrum.*, vol. 78, no. 4, p. 043 706, Apr. 2007.
[7] F. Goericke, J. Lee, and W. P. King, "Microcantilever hotplates with temperature-compensated piezoresistive strain sensors," *Sens. Actuators A, Phys.*, vol. 143, no. 2, pp. 181–190, May 2008.
[8] A. R. Krauss, O. Auciello, D. M. Gruen, A. Jayatissa, A. Sumant, J. Tucek, D. C. Macini, N. Moldovan, A. Erdemir, D. Ersoy, M. N. Gardos, H. G. Busmann, E. M. Meyer, and M. Q. Ding, "Ultrananocrystalline diamond thin films for MEMS and moving mechanical assembly devices," *Diamond Relat. Mater.*, vol. 10, no. 11, pp. 1952–1961, Nov. 2001.
[9] K. Shenai, R. S. Scott, and B. J. Baliga, "Optimum semiconductors for high-power electronics," *IEEE Trans. Electron Devices*, vol. 36, no. 9, pp. 1811–1823, Sep. 1989.
[10] E. Kohn, M. Adamschik, P. Schmid, A. Denisenko, A. Aleksov, and W. Ebert, "Prospects of diamond devices," *J. Phys. D, Appl. Phys.*, vol. 34, no. 16, pp. 77–85, Aug. 2001.
[11] W. Yang, O. Auciello, J. E. Butler, W. Cai, J. A. Carlisle, J. E. Gerbi, D. M. Gruen, T. Knickerbocker, T. L. Lasseter, J. N. Russell, Jr., L. M. Smith, and R. J. Hamers, "DNA-modified nanocrystalline diamond thin-films as stable, biologically active substrates," *Nat. Mater.*, vol. 2, no. 1, pp. 253–257, Jan. 2002.
[12] S. Jiao, A. Sumant, M. A. Kirk, D. M. Gruen, A. R. Krauss, and O. Auciello, "Microstructure of ultrananocrystalline diamond films grown by microwave Ar-CH_4 plasma chemical vapor deposition with or without added H_2," *J. Appl. Phys.*, vol. 90, no. 1, pp. 118–122, Jul. 2001.
[13] V. P. Adiga, A. V. Sumant, S. Suresh, C. Gudeman, O. Auciello, J. A. Carlisle, and R. W. Carpick, "Mechanical stiffness and dissipation in ultrananocrystalline diamond microresonators," *Phys. Rev. B, Condens. Matter*, vol. 79, no. 24, p. 245 403, Jun. 2009.
[14] A. V. Sumant, D. S. Grierson, J. E. Gerbi, J. A. Carlisle, O. Auciello, and R. W. Carpick, "Surface chemistry and bonding configuration of ultrananocrystalline diamond surfaces and their effects on nanotribological properties," *Phys. Rev. B, Condens. Matter*, vol. 76, no. 23, p. 235 429, 2007.
[15] S. Bhattacharyya, O. Auciello, J. Birrell, J. A. Carlisle, L. A. Crutiss, A. N. Goyette, D. M. Gruen, A. R. Krauss, J. Schlueter, A. Sumant, and P. Zapol, "Synthesis and characterization of highly-conducting nitrogen-doped ultrananocrystalline diamond films," *Appl. Phys. Lett.*, vol. 79, no. 10, pp. 1441–1443, Sep. 2001.
[16] X. Xiao, J. Birrell, J. E. Gerbi, O. Auciello, and J. A. Carlisle, "Low temperature growth of ultrananocrystalline diamond," *J. Appl. Phys.*, vol. 96, no. 4, pp. 2232–2239, Aug. 2004.
[17] W. S. Huang, D. T. Tran, J. Asmussen, T. A. Grotjohn, and D. Reinhard, "Synthesis of thick, uniform, smooth ultrananocrystalline diamond films

by microwave plasma-assisted chemical vapor deposition," *Diamond Relat. Mater.*, vol. 15, no. 2/3, pp. 341–344, Feb./Mar. 2006.
[18] M. A. Angadi, T. Watanabe, A. Bodapati, X. Xiao, O. Auciello, J. A. Carlisle, J. A. Eastman, P. Keblinski, P. K. Schelling, and S. R. Phillpot, "Thermal transport and grain boundary conductance in ultrananocrystalline diamond thin films," *J. Appl. Phys.*, vol. 99, no. 11, p. 114 301, Jun. 2006.
[19] M. Werner, P. Gluche, M. Adamschik, E. Kohn, and H.-J. Fecht, "Review of diamond based piezoresistive sensors," in *Proc. IEEE Int. Symp. Ind. Electron.*, 1998, vol. 1, pp. 147–152.
[20] J. L. Davidson, W. P. Kang, Y. Gurbuz, K. C. Holmes, L. G. Davis, A. Wisitsora-at, D. V. Kerns, R. L. Eidson, and T. Henderson, "Diamond as an active sensor material," *Diamond Relat. Mater.*, vol. 8, no. 8, pp. 1741–1747, Aug. 1999.
[21] M. Adamschik, R. Müller, P. Gluche, A. Flöter, W. Limmer, R. Sauer, and E. Kohn, "Analysis of piezoresistive properties of CVD-diamond films on silicon," *Diamond Relat. Mater.*, vol. 10, no. 9/10, pp. 1670–1675, Sep./Oct. 2001.
[22] P. Gluche, M. Adamschik, A. Vescan, W. Ebert, F. Szücs, H. J. Fecht, A. Flöter, R. Zachai, and E. Kohn, "Application of highly oriented, planar diamond (HOD) films of high mechanical strength in sensor technologies," *Diamond Relat. Mater.*, vol. 7, no. 6, pp. 779–782, Jun. 1998.
[23] O. Auciello, J. Birrell, J. A. Carlisle, J. E. Gerbi, X. Xiao, B. Peng, and H. D. Espinosa, "Materials science and fabrication processes for a new MEMS technology based on ultrananocrystalline diamond thin films," *J. Phys., Condens. Matter*, vol. 16, no. 16, pp. 539–552, Apr. 2004.
[24] P. Niedermann, W. Hänni, D. Morel, A. Perret, N. Skinner, P.-F. Indermühle, N.-F. de Rooij, and P.-A. Buffat, "CVD diamond probes for nanotechnology," *Appl. Phys. A, Solids Surf.*, vol. 66, no. S1, pp. S31–S34, 1998.
[25] W. L. Wang, X. Jiang, K. Taube, and C.-P. Klages, "Piezoresistivity of polycrystalline p-type diamond films of various doping levels at different temperatures," *J. Appl. Phys.*, vol. 82, no. 2, pp. 729–732, Jul. 1997.
[26] O. Dorsch, K. Holzner, M. Werner, E. Obermeier, R. E. Harper, C. Johnston, P. R. Chalker, and I. M. Buckley-Golder, "Piezoresistive effect of boron-doped diamond thin films," *Diamond Relat. Mater.*, vol. 2, no. 5–7, pp. 1096–1099, Apr. 1993.
[27] Y. Boiko, P. Gonon, S. Prawer, and D. N. Jamieson, "Piezoresistivity of boron doped CVD diamond films," *Mater. Sci. Eng. B*, vol. 46, no. 1–3, pp. 112–114, 1997.
[28] Y. Tang, D. M. Aslam, J. Wang, and K. D. Wise, "Study of polycrystalline diamond piezoresistive position sensors for application in cochlear implant probe," *Diamond Relat. Mater.*, vol. 15, no. 2/3, pp. 199–202, Feb./Mar. 2006.
[29] M. Aslam, I. Taher, A. Masood, M. A. Tamor, and T. J. Potter, "Piezoresistivity in vapor-deposited diamond films," *Appl. Phys. Lett.*, vol. 60, no. 23, pp. 2923–2925, Jun. 1992.
[30] J. Birrell, J. E. Gerbi, O. Auciello, J. M. Gibson, J. Johnson, and J. A. Carlisle, "Interpretation of the Raman spectra of ultrananocrystalline diamond," *Diamond Relat. Mater.*, vol. 14, no. 1, pp. 86–92, Jan. 2005.
[31] O. A. Williams, M. Daenen, J. D'Haen, K. Haenen, J. Maes, V. V. Moshchalkov, M. Nesládek, and D. M. Gruen, "Comparison of the growth and properties of ultrananocrystalline diamond and nanocrystalline diamond," *Diamond Relat. Mater.*, vol. 15, no. 4–8, pp. 654–658, Apr.–Aug. 2006.
[32] J. E. Gerbi, O. Auciello, J. Birrell, D. M. Gruen, B. W. Alphenaar, and J. A. Carlisle, "Electrical contacts to ultrananocrystalline diamond," *Appl. Phys. Lett.*, vol. 83, no. 10, pp. 2001–2003, Sep. 2003.
[33] R. G. Budynas, *Advanced Strength and Applied Stress Analysis,* 2nd ed. New York: McGraw Hill, 1999.
[34] L. J. van der Pauw, "A method of measuring the resistivity and Hall coefficient on lamellae of arbitrary shape," *Philips Tech. Rev.*, vol. 20, pp. 220–224, 1958.
[35] M. Werner and R. Locher, "Growth and application of undoped and doped diamond films," *Rep. Prog. Phys.*, vol. 61, no. 12, pp. 1665–1710, Dec. 1998.
[36] W. Gajewski, P. Achatz, O. A. Williams, K. Haenen, E. Bustarret, M. Stutzmann, and J. A. Garrido, "Electronic and optical properties of boron-doped nanocrystalline diamond films," *Phys. Rev. B, Condens. Matter*, vol. 79, no. 4, p. 045 206, Jan. 2009.
[37] P. French and A. Evans, *Properties of Silicon (EMIS Datareviews Series No. 4).* New York: INSPEC, 1988, ch. 3.4, pp. 94–103.

Natalya L. Privorotskaya received the B.S. and M.S. degrees in mechanical engineering from Rochester Institute of Technology, Rochester, NY, in 2005, and the Ph.D. degree in mechanical engineering from the University of Illinois at Urbana–Champaign, Urbana, in 2009, where her dissertation focused on the development, fabrication, and characterization of silicon and ultrananocrystalline diamond cantilever sensors for biochemical detection.

She is currently with Intel, Chandler, AZ.

Hongjun Zeng (M'05–SM'06) received the B.S. and M.S. degrees in optics from Sichuan University, Chengdu, China, in 1994 and 1997, respectively, and the Ph.D. degree in optical engineering from the Institute of Optics and Electronics, Chinese Academy of Sciences, Chengdu, in 2000.

He is currently a Senior MEMS R&D Scientist with Advanced Diamond Technologies, Inc., Romeoville, IL. He is the author/coauthor of more than 60 research papers and patents/disclosures. His research interests include chemical vapor deposition synthesis of diamond films and their applications, micro- and nanofabrications, devices, and materials.

John A. Carlisle received the Ph.D. degree in physics from the University of Illinois at Urbana–Champaign, Urbana, in 1993.

He is currently the Chief Technical Officer of Advanced Diamond Technologies, Inc., Romeoville, IL, which he cofounded in 2003. From 2000 to 2006, he was a Staff Scientist in the Materials Science Division, Argonne National Laboratory. For the past 15 years, his interests have focused on the synthesis, properties, and application of nanostructured carbon materials in products ranging from low-friction wear-resistant coatings to biosensors, RF electronics, and other devices made using diamond-based MEMS technology.

Dr. Carlisle is a member of the Materials Research Society and American Physical Society. He is a three-time recipient of the R&D100 Award. In 2006, he received an Excellence in Technology Transfer Award from the Federal Laboratory Consortium and was recognized as a Technology Pioneer by the World Economic Forum in 2007.

Rashid Bashir (F'09) received the Ph.D. degree from Purdue University, West Lafayette, IN, in 1992.

From October 1992 to 1998, he was with the Analog/Mixed Signal Process Technology Development Group, National Semiconductor, where he became a Senior Engineering Manager. He joined Purdue University in October 1998 as an Assistant Professor and became a Professor of electrical and computer engineering and a Courtesy Professor of biomedical engineering and mechanical engineering. Since October 2007, he has been the Abel Bliss Professor of Electrical and Computer Engineering and Bioengineering and the Director of the Micro and Nanotechnology Laboratory (a campus-wide clean room facility), University of Illinois at Urbana–Champaign, Urbana. He has authored or coauthored over 100 journal papers, over 130 conference papers and abstracts, and over 70 invited talks. He is the holder of 34 patents. His research interests include BioMEMS, lab on a chip, nanobiotechnology, interfacing biology and engineering from molecular to tissue scale, and applications of semiconductor fabrication to biomedical engineering, which are all applied to solve biomedical problems.

Dr. Bashir is a Fellow of the American Institute of Medical and Biological Engineers.

William P. King (M'04) received the B.S. degree from the University of Dayton, Dayton, OH, in 1996, and the M.S. and Ph.D. degrees from Stanford University, Stanford, CA, in 1998 and 2002, respectively, all in mechanical engineering.

He is a Professor and a Willett Faculty Scholar in the Departments of Mechanical Science and Engineering and Materials Science and Engineering, University of Illinois at Urbana–Champaign (UIUC), Urbana. From 1999 to 2001, he was with the Micro/NanoMechanics Group, IBM Zurich Research Laboratory. From 2002 to 2006, he was with the faculty of Georgia Institute of Technology, Atlanta. At UIUC, his group works on nanometer-scale thermal and mechanical measurements, engineering of nanomechanical devices, and micro- and nanomanufacturing. He is the cofounder of two companies.

Dr. King was the recipient of a CAREER Award from the National Science Foundation in 2003, PECASE Award from the Department of Energy in 2005, Young Investigator Award from the Office of Naval Research in 2007, ASME Bergles–Rohsenow Young Investigator Award in Heat Transfer in 2009, and two R&D 100 Awards. He was named as the Young Manufacturing Engineer by the Society of Manufacturing Engineers in 2006. In 2006, *Technology Review Magazine* named him to the TR35—one of the people under the age of 35 whose innovations are likely to change the world. He is a member of the Defense Sciences Research Council.